RhoA GTPase controls cytokinesis and programmed necrosis of hematopoietic progenitors

Xuan Zhou,[1,2] Maria Carolina Florian,[5] Paritha Arumugam,[1] Xiaoyi Chen,[1] Jose A. Cancelas,[1,2] Richard Lang,[2,3,4] Punam Malik,[1] Hartmut Geiger,[1,2,5] and Yi Zheng[1,2]

[1]Division of Experimental Hematology and Cancer Biology, [2]Molecular and Development Biology Graduate Program, [3]Division of Ophthalmology, and [4]Division of Developmental Biology, Cincinnati Children's Research Foundation, University of Cincinnati, Cincinnati, OH 45229
[5]Department of Dermatology and Allergic Diseases, University of Ulm, 89075 Ulm, Germany

Hematopoietic progenitor cells (HPCs) are central to hematopoiesis as they provide large numbers of lineage-defined blood cells necessary to sustain blood homeostasis. They are one of the most actively cycling somatic cells, and their precise control is critical for hematopoietic homeostasis. The small GTPase RhoA is an intracellular molecular switch that integrates cytokine, chemokine, and adhesion signals to coordinate multiple context-dependent cellular processes. By using a *RhoA* conditional knockout mouse model, we show that *RhoA* deficiency causes a multilineage hematopoietic failure that is associated with defective multipotent HPCs. Interestingly, *RhoA*$^{-/-}$ hematopoietic stem cells retained long-term engraftment potential but failed to produce multipotent HPCs and lineage-defined blood cells. This multilineage hematopoietic failure was rescued by reconstituting wild-type RhoA into the *RhoA*$^{-/-}$ Lin^{-}Sca-1^{+}c-Kit^{+} compartment. Mechanistically, RhoA regulates actomyosin signaling, cytokinesis, and programmed necrosis of the HPCs, and loss of *RhoA* results in a cytokinesis failure of HPCs manifested by an accumulation of multinucleated cells caused by failed abscission of the cleavage furrow after telophase. Concomitantly, the HPCs show a drastically increased death associated with increased TNF–RIP-mediated necrosis. These results show that RhoA is a critical and specific regulator of multipotent HPCs during cytokinesis and thus essential for multilineage hematopoiesis.

CORRESPONDENCE
Yi Zheng:
yi.zheng@cchmc.org

Abbreviations used: 5-FU, fluorouracil; CFC, colony-forming cell; cKO, conditional KO; HPC, hematopoietic progenitor cell; HSC, hematopoietic stem cell; HSPC, hematopoietic stem and progenitor cell; IMDM, Iscove's modified Dulbecco's medium; mDia, mammalian diaphanous; MLC, myosin light chain; PB, peripheral blood; RIP, receptor-interacting protein kinase; ROCK, Rho-associated kinase; SCF, stem cell factor.

Mammalian hematopoiesis is a hierarchical and highly dynamic process (Ghaffari, 2008). This rapid and regulated program is sustained by a rare population of relatively quiescent hematopoietic stem cells (HSCs) that continuously generate hematopoietic progenitor cells (HPCs). HPCs are the workhorses in hematopoiesis and are critical for homeostasis of the blood system, as they are primarily responsible for the expansion of HSC progenies and generating differentiated blood cells. HPCs are therefore endowed with a very high proliferation potential. Consequently, a precise yet flexible regulatory program of HPC division is crucial to the maintenance of blood cell homeostasis under normal and stress conditions, the malfunction of which can cause a variety of hematologic diseases including BM failure, anemia, leukemia, and lymphoma (Boggs and Boggs, 1976; Bonnet and Dick, 1997; Castor et al., 2005). Thus, elucidating the mechanisms governing HPC proliferation and differentiation is of great significance.

The homeostasis of hematopoietic stem and progenitor cells (HSPCs) relies on, among other mechanisms, tightly controlled cell cycle and survival machineries. Molecules involved in regulating the cell cycle, such as p16^{Ink4A}, p21$^{Cip1/Waf1}$, p27^{Kip1}, PTEN, and Egr1, and those regulating cell survival and apoptosis, such as p53, Bcl2, Bcl-x, and Mcl1, are essential for the maintenance of HSPCs (Cheng et al., 2000a,b; Arai et al., 2004; Kozar et al., 2004; Janzen et al., 2006;

The Rockefeller University Press $30.00
J. Exp. Med. 2013 Vol. 210 No. 11 2371-2385
www.jem.org/cgi/doi/10.1084/jem.20122348

Yilmaz et al., 2006; Zhang et al., 2006; Min et al., 2008; Zou et al., 2011). However, a more detailed picture of the machinery governing cell cycle progression, especially how cytokinesis is regulated during hematopoiesis, is currently not available. Cytokinesis is central for determining the identities of daughter cells upon division because it separates genetic materials, patterns cytosolic cell fate determinants, and determines the relative positions of the daughter cells to the niche (Knoblich, 2008). Mitotic failure can lead to aneuploidy and genomic instability, which may result in cell death (Castedo et al., 2004a) or transformation (Storchova and Pellman, 2004; Ganem et al., 2007). In addition, because HSCs and HPCs are different in proliferative kinetics, distinct cytokinesis machineries might be essential to maintain a relative quiescent stem cell pool and an actively dividing progenitor population. Defining regulatory mechanisms of cytokinesis of primitive hematopoiesis cells, and understanding mechanistic relationships between cell cycle abnormalities and cell death control, may result in more detailed knowledge of the regulatory machineries for critical steps in hematopoiesis.

Ras homologue gene family, member A (RhoA) is among the first members of the Rho GTPase family identified and is best known as a critical regulator of cytoskeleton dynamics. It cycles between the GTP-bound active and GDP-bound inactive forms in response to diverse cellular stimuli under tight regulation (Van Aelst and D'Souza-Schorey, 1997). Upon activation (i.e., RhoA-GTP), RhoA transduces signals to downstream effectors to elicit cell functions including cell adhesion, survival, cell cycle progression, and transcription; studies have reported a critical involvement of RhoA in regulating cytokinesis (Jaffe and Hall, 2005). Active RhoA and its downstream signaling components such as F-actin, myosin, and annilin are concentrated at the cleavage furrow during cytokinesis. Disruption of this process results in cytokinesis failure and multinucleated cells (Piekny et al., 2005). However, our current knowledge about RhoA function is mostly derived from dominant-negative or constitutively active mutant overexpression studies performed in cultured cell lines, which are limited by specificity and dosage issues in their physiological implications. Models in which *RhoA* is genetically deleted are better systems to define the role of RhoA in tissue/cell type–specific physiological conditions. To this end, several recent conditional gene-targeting studies in mouse models have begun to reveal the unique and important functions of RhoA in various mammalian organs (Geh et al., 2011; Jackson et al., 2011; Melendez et al., 2011; Xiang et al., 2011; Pleines et al., 2012; Zhang et al., 2012). It appears that RhoA signaling function is cell type and pathway dependent, and many previously suggested cellular roles of RhoA may not be applicable to complex biological processes in vivo.

In this study, we investigate the role of RhoA in regulating HSPCs and hematopoiesis using an inducible *RhoA* conditional KO (cKO) model (*Mx-cre*, $RhoA^{fl/fl}$). We demonstrate that RhoA is essential for multilineage hematopoiesis and deletion of *RhoA* results in acute pancytopenia and BM failure. In the HSPC compartment, *RhoA* deficiency does not affect stem cell engraftment but significantly impairs the function of multipotent progenitor cells. *RhoA*-null HPCs exhibit a cytokinesis block and undergo programmed necrosis but not apoptosis. Our results suggest for the first time that programmed necrosis associated with a cytokinesis arrest is an underlying mechanism of maintaining HPC homeostasis.

RESULTS

RhoA is essential for multilineage hematopoiesis

RhoA mRNA is expressed in the HSC and the progenitor (multipotent progenitor, $Lin^-Sca\text{-}1^-c\text{-}kit^+$ [LK]) compartments of the BM cells (not depicted). Biochemically, RhoA GTPase cycles between a GDP-bound inactive form and a GTP-bound active form. To examine the physiological relevance of RhoA activity, we used a Rhotekin pull-down assay to monitor relative RhoA-GTP level in response to stimuli known to activate HSPCs, including stem cell factor (SCF), stromal cell–derived factor 1α (SDF-1α), and fibronectin (Yoder and Williams, 1995; Broudy, 1997; Hattori et al., 2003). We observed that these factors all led to a substantial increase of GTP-bound active RhoA in lineage-negative (Lin^-) cells (Fig. 1 A), suggesting that RhoA signaling is active and likely involved in regulating primitive hematopoietic cells in response to these hematopoietic regulatory factors.

To examine the relevance of RhoA signaling in stress-induced hematopoiesis, we examined RhoA activity in response to fluorouracil (5-FU) treatment, which was a strong myeloablative reagent and could induce massive HSPC proliferation (Randall and Weissman, 1997; Venezia et al., 2004). 5-FU treatment caused a significant increase of RhoA activity in BM low-density monocytes without altering RhoA protein expression (Fig. 1 B). To further examine the activity of RhoA signaling within the hematopoietic progenitors, we measured the phosphorylation of regulatory myosin light chain (MLC), which is regulated by RhoA downstream effectors Rho-associated kinase (ROCK) and citron kinase (Kimura et al., 1996; Maekawa et al., 1999; Yamashiro et al., 2003). Increased phosphorylation of MLC was observed during the transition from the more primitive $Lin^-Sca\text{-}1^+$ $c\text{-}Kit^+$ (LSK) to the less primitive LK populations (Fig. 1 C). In addition, in the HSC-enriched $Lin^-CD150^+CD48^-$ (SLAM) population (Kiel et al., 2005), RhoA signaling in response to 5-FU treatment, monitored by the phosphorylation of MLC, closely correlated with the proliferative status of HSC (Fig. 1 D; Randall and Weissman, 1997; Venezia et al., 2004). Together these results suggest that RhoA activity is associated with the function hematopoietic progenitors.

To determine the function of RhoA in HSPCs, we crossed the interferon-inducible *Mx-cre* mice (Kühn et al., 1995) with $RhoA^{fl/fl}$ mice (Melendez et al., 2011) and induced deletion of *RhoA* using synthetic double-strand RNA poly I:C. Lin^- cells isolated from *Mx-cre*$^+$; $RhoA^{fl/fl}$ mice (*RhoA*-cKO) exhibited efficient RhoA deletion 3 d after two poly I:C injections (Fig. 1, E and F), and *RhoA* deletion did not cause a compensatory overexpression of the closely related Rho GTPase RhoB or RhoC (Fig. 1 F and not depicted). Interestingly, deletion of

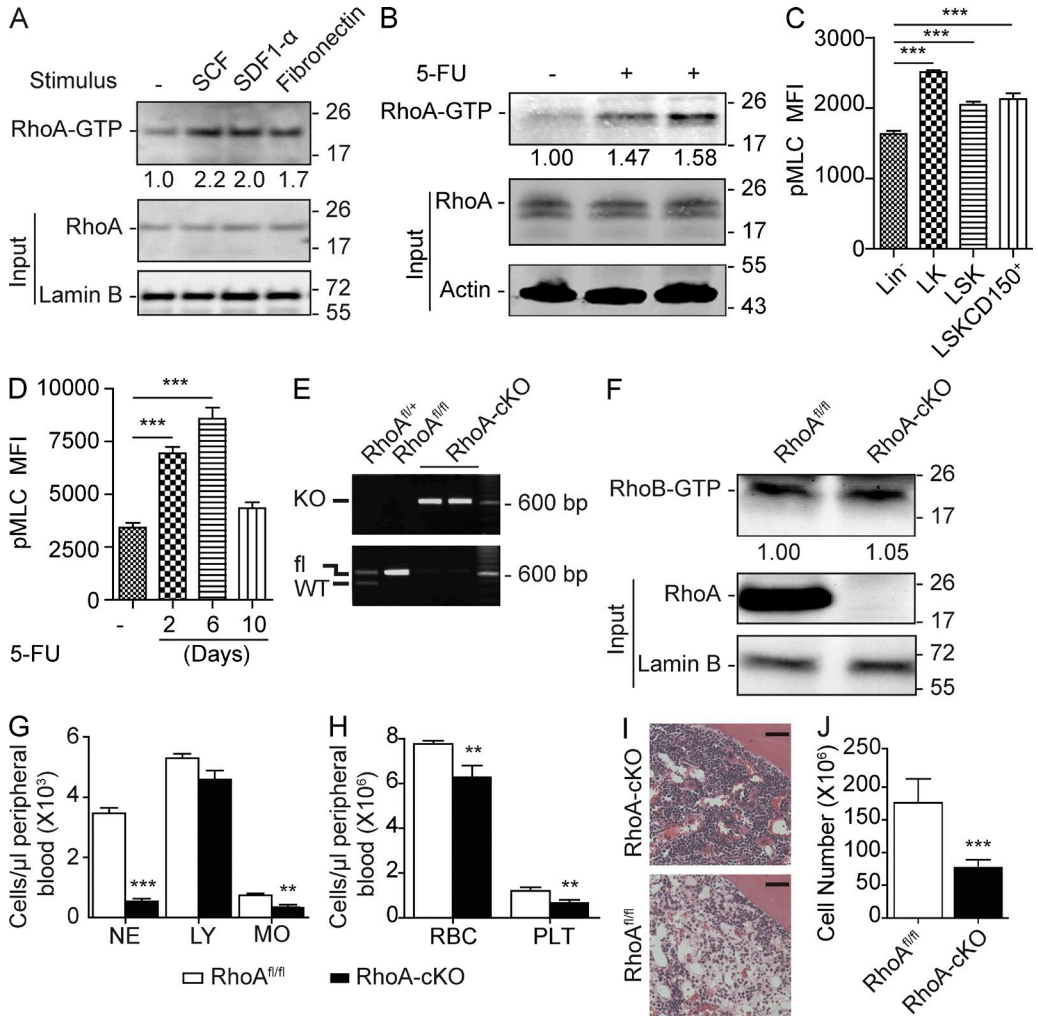

Figure 1. ***RhoA*** **deficiency causes acute hematopoietic failure.** (A) Isolated Lin$^-$ cells were stimulated with SCF, SDF-1α, and fibronectin, and relative RhoA activity was determined by normalizing to total RhoA input. (B) Low-density monocytes were isolated 6 d after 5-FU injection, and relative RhoA activity was normalized to total RhoA input. (C) Phosphorylation of MLC (Ser19) in the WT primitive HSPC populations was determined by flow cytometry. MFI, mean fluorescence intensity. (D) Kinetics of MLC phosphorylation (Ser19) in Lin$^-$SLAM population after 5-FU treatment was determined by flow cytometry. (E) *RhoA* deletion efficiency of the *Mx-cre*$^+$*RhoA*$^{fl/fl}$ mice was determined by genotyping PCR using Lin$^-$ cells 3 d after induction. (F) RhoB activity was assessed using Lin$^-$ cells isolated 3 d after poly I:C induction. RhoB activity was determined and normalized against Lamin B. (G and H) PB counts of the congenic transplantation recipients. CD45.2$^+$ *RhoA*$^{fl/fl}$; *Mx-cre*$^+$ or *Mx-cre*$^-$ cells were transplanted into lethally irradiated CD45.1$^+$ WT recipients. Three poly I:C injections were administrated 2 mo after transplantation. Recipients were sacrificed for analysis at 5 d after the last poly I:C injections. NE, neutrophils; LY, lymphocytes; MO, monocytes; RBC, red blood cells; PLT, platelets. (I) Representative H&E staining of femur sections. Bars, 40 μm. (J) Absolute number of BM white cells in the tibia, femur, and iliac crest 5 d after three poly I:C injections. Numbers of samples analyzed: four (C and D) or five (G, H, and J) per group. (A–D, F–H, and J) The results from a representative experiment of two independent experiments are shown. (A, B, and F) Molecular masses (kilodaltons) are indicated to the right of the blots. Error bars indicate SEM. **, $P < 0.01$; ***, $P < 0.001$.

the floxed allele in the BM of *Mx-Cre*$^+$; *RhoA*$^{fl/+}$ heterozygous mice did not affect RhoA protein expression nor cause detectable hematopoietic defects (not depicted).

Although the *Mx-cre*–mediated gene targeting models have been broadly used in hematopoietic studies, gene KO is not limited to the blood system (Kühn et al., 1995). To specifically delete *RhoA* from the hematopoietic lineages, we induced *RhoA* deletion after transplantation of BM cells from *Mx-cre*$^+$; *RhoA*$^{fl/fl}$ mice into congenic CD45.1$^+$ recipients. The recipients presented with multilineage cytopenia in response to *RhoA* deletion and died 1 wk after poly I:C induction. By 5 d after poly I:C injections, *RhoA* deficiency resulted in a rapid and significant decrease of neutrophils (0.54 ± 0.09 k/μl in *RhoA*-cKO mice vs. 3.64 ± 0.18 k/μl in control) and a significant reduction of monocytes and platelets in the peripheral blood (PB; Fig. 1, G and H). In the erythroid lineage, *RhoA* deficiency resulted in a small but significant reduction of red blood cells (Fig. 1 H). *RhoA* deficiency did not alter the count of circulating lymphocytes in this experimental set-up (Fig. 1 G), as these lineages usually posed a longer life span

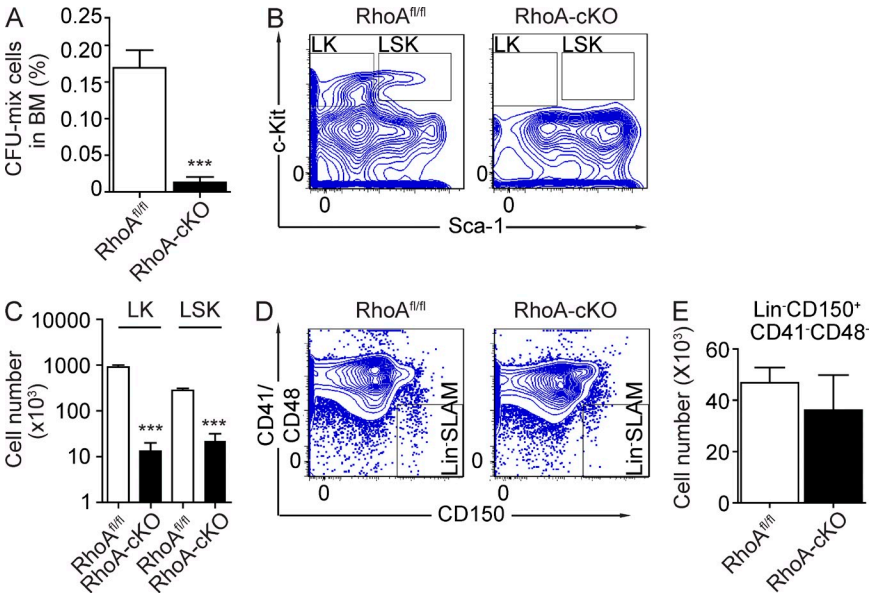

Figure 2. *RhoA* deficiency reduces hematopoietic progenitors but not HSCs. (A) Frequency of CFCs in BM 5 d after poly I:C treatments. (B and C) Number of LK and LSK cells in BM 5 d after poly I:C treatments. (B) Representative flow cytometry plots of BM LK and LSK populations. (C) Quantification of LK and LSK cell numbers in tibia, femur, and iliac crest. (D and E) The number of Lin$^-$SLAM cells in BM. (D) Representative flow cytometry plots of the Lin$^-$SLAM population. (E) Quantification of the number of Lin$^-$SLAM cells in tibia, femur, and iliac crest. All mice used in this figure were congenic transplantation recipients as described in Fig. 1 G. Numbers of samples analyzed: five per group (A and C) and four (*RhoA*$^{fl/fl}$) and five (*RhoA*-cKO; E). (A–E) The results from a representative experiment of two independent experiments are shown. Error bars indicate SEM. ***, $P < 0.001$.

than the relatively short time course (1 wk) of this experiment. Subsequent competitive transplantation experiments, though, showed that *RhoA* was also critical for the development of lymphocytes (see Fig. 3, C and D).

Consistent with decreased number of cells in the periphery, we observed a significant reduction of BM cellularity. Hematoxylin and eosin (H&E) histology examination showed a drastic reduction of major blood cell types, including both myeloid and erythroid cells (Fig. 1 I). Consistently, total white blood cells in tibia, femur, and iliac crest in *RhoA*-cKO mice were reduced from $176.2 \pm 16.2 \times 10^6$ to $77.0 \pm 5.5 \times 10^6$ (Fig. 1 J). Thus, *RhoA* deficiency results in acute multilineage cytopenia and a BM failure.

RhoA deficiency results in a loss of multilineage HPCs

Because *RhoA* loss reduced multiple blood lineages, we hypothesized that RhoA signaling is critical for maintaining HSPCs. To test this hypothesis, we initially performed colony-forming cell (CFC) assays to examine in vitro progenitor activities. *RhoA* deficiency dramatically reduced the BM content of CFCs 5 d after poly I:C induction ($0.013 \pm 0.008\%$ in *RhoA*-cKO mice compared with $0.170 \pm 0.024\%$ in control mice, $P < 0.001$; Fig. 2 A). Consistent with this result, we also observed a significant reduction of primitive LSK cells and less primitive progenitor LK cells in the *RhoA*-cKO BM revealed by FACS analysis (Fig. 2, B and C). Because CD150$^+$CD41$^-$CD48$^-$ (SLAM) cells are enriched for primitive HSC activities (Kiel et al., 2005), we also checked whether *RhoA* deficiency also altered Lin$^-$CD150$^+$CD41$^-$CD48$^-$ (Lin$^-$SLAM) cells in the BM. The numbers of Lin$^-$SLAM cells in *RhoA*-cKO mice were comparable with controls (Fig. 2, D and E), suggesting that RhoA activity might not be required for HSC maintenance. Thus, loss of RhoA depletes the functionally and phenotypically defined hematopoietic progenitors, yet phenotypically identified HSCs appear preserved in *RhoA*-cKO BM.

RhoA is required for hematopoietic homeostasis in competitive transplantation

In *RhoA*-cKO mice, severe HPC loss correlates with an acute reduction of differentiated hematopoietic cells. The loss of progenitor cells may be causal for the loss of mature cells. However, it is also possible that the loss of mature cells may lead to a feedback exhaustion of progenitors. In addition, although phenotypic HSCs are preserved in the *RhoA*-cKO mice, we could not determine the long-term functionality of the HSCs using the previous model as a result of the rapid death of *RhoA*-cKO mice after poly I:C inductions. A competitive transplantation experiment could address these concerns because of the presence of WT competitor cells, thus avoiding compensational activation/exhaustion of progenitors and sustaining the survival of the recipients to allow long-term functional analysis of donor HSCs, including secondary transplants.

Consistent with the data from the noncompetitive transplantation experiment, upon deletion of *RhoA* we observed a rapid and persistent reduction of donor-derived (*RhoA*$^{-/-}$, CD45.2$^+$) blood cells in the peripheral circulation in the competitive transplant model. This reduction was observed in all major blood lineages (myeloid, T, and B cell lineages; Fig. 3), demonstrating that the hematopoietic-autonomous absence of *RhoA* impairs multilineage hematopoiesis.

RhoA is essential for HPC activity but is dispensable for the maintenance of HSCs

To study the functionality of *RhoA*-null HSCs and progenitors, we examined the frequency of donor-derived (CD45.2$^+$) LSK and LK cells in the competitive transplantation model. We found that *RhoA*-deficient LK cells were not capable of competing with competitor cells. 5 mo after secondary transplantation, the percentage of donor derived (CD45.2$^+$) LK cells dropped to 15% of the original (Fig. 4, A and B). In contrast, deletion of *RhoA* did not significantly affect the more

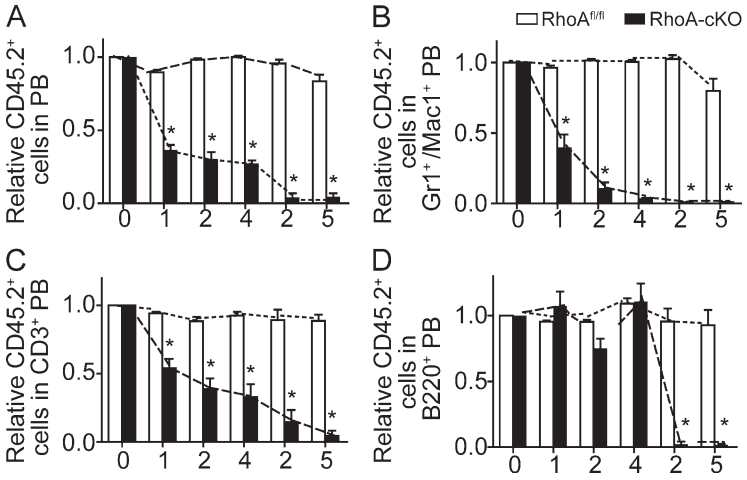

Figure 3. *RhoA* deficiency impairs multilineage hematopoiesis in a competitive transplantation experiment. (A–D) Lethally irradiated CD45.1+ recipient mice were reconstituted with equal numbers of CD45.2+ donor BM cells of the *RhoA*$^{fl/fl}$*Mx-cre*$^{+}$ or *Mx-cre*$^{-}$ genotype with CD45.1+ WT competitors. Three poly I:C injections were administrated into the recipients 8 wk after transplantation, and the chimerism of PB was analyzed monthly thereafter. 4 mo after poly I:C inductions, BM cells from the primary recipients were pooled and transplanted into secondary recipients. The kinetics of relative chimerism of donor-derived (CD45.2+) cells in total PB (A), myeloid (B), T (C), and B (D) cells in the peripheral circulation of recipients are shown. The x axes show units in months. Months 0–4: primary recipients; months 2–5: secondary recipients. Seven mice per genotype were examined. The results from a representative experiment of three independent experiments are shown. Error bars indicate SEM. *, $P < 0.001$.

primitive LSK population. The frequency of *RhoA*-null LSK cells was not significantly different from the control group, and more importantly, they were capable of engrafting into secondary recipients (Fig. 4, A and C). Efficient deletion of *RhoA* in the donor-derived (CD45.2+) LSK population was confirmed by PCR (Fig. 4 E). Furthermore, loss of *RhoA* did not alter the frequency of CD45.2+ cells in the HSC-enriched LSKCD150+ population (93.3 ± 18.0% in the *RhoA*-cKO group compared with 99.4 ± 4.0% in control mice; Kiel et al., 2005), indicating that *RhoA* might be dispensable for long-term HSC maintenance (Fig. 4, A and D).

To formally demonstrate the functionality of *RhoA*-null phenotypic HSCs, we performed a rescue experiment to see whether expressing RhoA in *RhoA*$^{-/-}$ LSK cells was able to restore multilineage hematopoiesis. We isolated LSK cells from poly I:C–injected competitive transplanted recipients and transduced them with lentivirus expressing human *RhoA* cDNA or control virus. These viruses also expressed eGFP as a reporter for transduction. The cells were transplanted into lethally irradiated CD45.1+ recipients without purifying for the eGFP+ cells. Contributions of corrected *RhoA*$^{-/-}$ cells to hematopoiesis were determined by percentage of CD45.2+ cells within the eGFP+ populations. Transduction with RhoA-expressing lentivirus, not the control virus, was able to completely rescue the multilineage differentiation defects of the *RhoA*$^{-/-}$ LSK donor cells. The percentages of CD45.2+Gr-1+ myeloid cells, B220+ B cells, and CD3e+ T cells within RhoA lentivirus–transduced *RhoA*$^{-/-}$ group were comparable with that of the *RhoA*$^{fl/fl}$ groups transduced with either RhoA or control virus, whereas little or no CD45.2+ myeloid, B, or T cells were observed in the control virus–transduced *RhoA*$^{-/-}$ group (Fig. 4 F), indicating that the *RhoA*$^{-/-}$ LSK cell population still contained HSC activity. Because hematopoiesis was sustained by WT competitor cells in the competitive transplant model, these phenotypes reflected the HSC-intrinsic effects of *RhoA* deficiency. The results show that *RhoA* is absolutely required in HPCs but, surprisingly, is dispensable for maintaining HSCs.

RhoA deficiency reduces actomyosin signaling and SDF-1α–driven chemotaxis

As shown in Figs. 1 and 2, by 5 d after poly I:C injections, *RhoA*-deficient hosts suffered a severe pan-cytopenia and BM failure, making this later time point unsuitable for mechanistic interpretation of RhoA signaling. To investigate the mechanism associated with the loss of HPCs upon *RhoA* gene deletion, we performed a time course study to identify the earliest time point at which RhoA was efficiently removed from Lin− BM cells. A reduction of RhoA protein was observed 2 d after poly I:C injections, but a complete KO of RhoA was not achieved until 3 d after injections (not depicted). Therefore, we chose to use mice 3 d after poly I:C injections for the following experiments.

RhoA is involved in regulating cellular adhesion and migration, which are relevant to HSPC niche residency and maintenance (Yoder and Williams, 1995). Multiple molecular players in these pathways are regulated by RhoA. RhoA is a critical regulator of actomyosin activity, primarily through its downstream effectors ROCK (Kimura et al., 1996; Maekawa et al., 1999) and citron kinase (Yamashiro et al., 2003). Consistent with previous studies in other tissues (Chauhan et al., 2011; Jackson et al., 2011), *RhoA* deficiency led to a dramatic reduction of phosphorylated MLC in the isolated Lin− cells (Fig. 5 A), suggesting a deficiency in actomyosin machinery in the HPC population. In addition to p-MLC regulation, RhoA is also known to be a critical factor in regulating actin microfilament polymerization/stability through regulating mammalian diaphanous (mDia) and ROCK (Jaffe and Hall, 2005). Surprisingly, cofilin activity, which destabilizes actin filament, was unchanged after *RhoA* deletion (Fig. 5 B). Actin polymerization was increased, rather than reduced, in *RhoA*-deficient cells (Fig. 5, C and D). *RhoA* deficiency also led to an ∼50% reduction of SDF-1α–driven chemotaxis (Fig. 5 E), consistent with the reduced p-MLC activity (Fig. 5 A). Unexpectedly, *RhoA* loss increased, rather than decreased, the adhesion of Lin− cells to a fibronectin-coated surface (Fig. 5 F). It is unlikely that changes in the pathways regulating adhesion

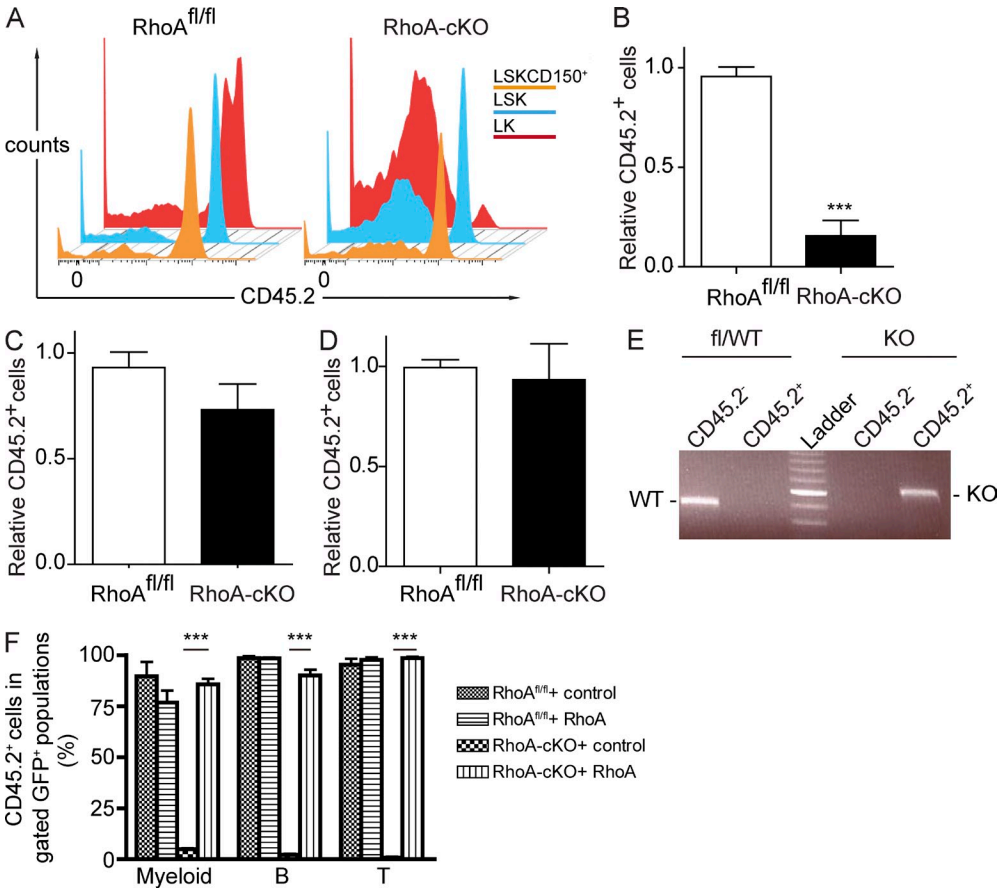

Figure 4. *RhoA* deficiency depletes HPCs but not HSCs in competitive setting. (A) CD45.2$^+$ donor BM cells of the *RhoA*$^{fl/fl}$*Mx-cre*$^+$ or *Mx-cre*$^-$ genotype were cotransplanted into lethally irradiated CD45.1$^+$ recipients together with equal number of CD45.1$^+$ WT competitor cells. Three poly I:C injections were administrated 8 wk after the transplantation, and BM cells from the primary recipients were transplanted into secondary recipients 4 mo after the poly I:C injections. Data were analyzed 5 mo after secondary transplantation. Representative flow cytometry plots of CD45.2 expression within the LK, LSK, and LSKCD150$^+$ population in the competitive transplant recipients are shown. (B–D) Relative chimerism of donor-derived LK (B), LSK (C), and LSKCD150$^+$ (D) in BM of recipients. (E) DNA from sorted CD45.2$^+$ LSK cells was used as PCR template to determine the deletion efficiency of RhoA. Data were analyzed 5 mo after secondary transplantation. Brightest band of ladder: 600 bp. (F) LSK cells from poly I:C–injected competitive transplantation recipients were transduced with RhoA-expressing or control virus and transplanted into secondary recipients. PB samples were examined 16 wk after transplantation. Percentage of donor-derived (CD45.2$^+$) cells in gated GFP$^+$ mature lineages of PB was determined by flow cytometry. Numbers of mice analyzed: six (A–D) and four (F) mice per group. The results from a representative experiment of three (A–D) or two (F) independent experiments are shown. Error bars indicate SEM. ***, $P < 0.001$.

and migration are the primary driving force in loss of HPCs and HPC differentiation in response to RhoA deficiency.

RhoA regulates cytokinesis of HPCs through the ROCK and mDia pathways

A previous study has shown that suppression of RhoA via a dominant-negative mutant approach results in increased HSPC proliferation and engraftment (Ghiaur et al., 2006). However, recent studies in Rho GTPases have revealed that overexpression of dominant-negative mutants may produce nonspecific biological responses as a result of the inherent nonspecific biochemical function of the mutants that are capable of sequestering multiple endogenous Rho-, Rac-, and/or Cdc42-activating guanine nucleotide exchange factors (Wang and Zheng, 2007; Heasman and Ridley, 2008). To examine whether *RhoA* deficiency alters cell proliferation in our genetic deletion model, we performed a BrdU incorporation assay to determine the distribution of *RhoA*$^{-/-}$ cells in the distinct stages of the cell division cycle (G_0/G_1 and S, G_2/M phase). In the noncompetitive transplantation model, a significant increase of BrdU$^+$ cells in both LSK and LK populations was observed 3 d after poly I:C induction (Fig. 6 A). However, the increased proliferation in this model is likely a secondary effect caused by the acute hematopoietic stress seen upon RhoA deletion. We observed no change in BrdU incorporation when cells from the competitive transplantation recipients were analyzed, which served as a homeostatic hematopoiesis model (Fig. 6 B). These results indicate that RhoA is not essential for regulating the G_1/S transition of steady-state hematopoietic progenitors.

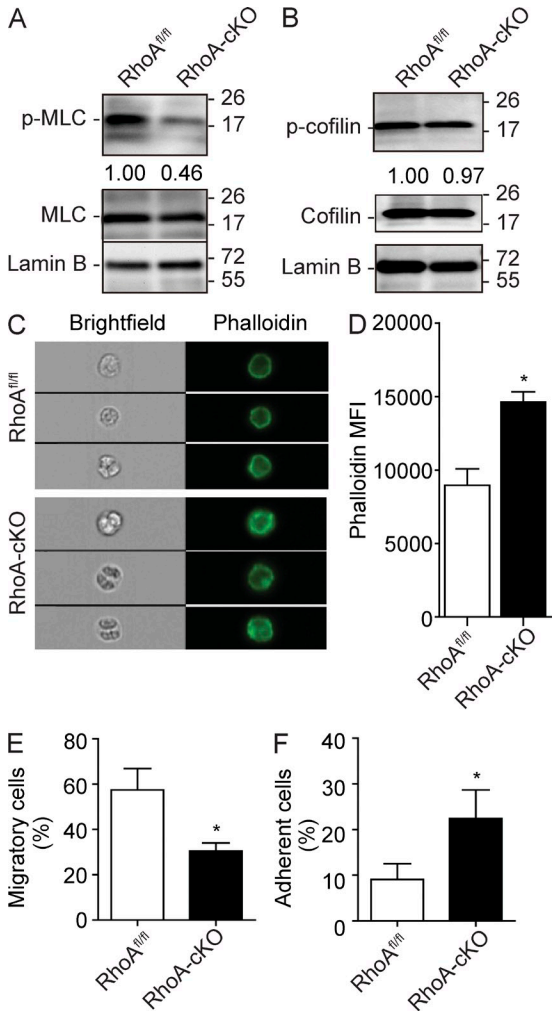

Figure 5. RhoA regulates HSPC actomyosin signaling, migration, and adhesion. (A) MLC phosphorylation (Ser19) in Lin$^-$ BM cells 3 d after poly I:C induction. Relative MLC phosphorylation was determined by normalizing to total MLC expression. (B) Cofilin (Ser3) phosphorylation in isolated Lin$^-$ BM cells 3 d after poly I:C induction. Relative cofilin phosphorylation was determined by normalizing to total cofilin. (A and B) Molecular masses (kilodaltons) are indicated to the right of the blots. (C and D) Cortical F-actin formation in response to 100 ng/ml SDF-1α stimulation in Lin$^-$ cells. Lin$^-$ cells were isolated from mice 3 d after induction and stained with Alexa Fluor 488 phalloidin. (C) Representative ImageStream images of F-actin staining in Lin$^-$ cells. (D) Quantification of cortical F-actin signaling. MFI, mean fluorescence intensity. (E) Lin$^-$ BM cells were cultured in the top chamber of Transwells. 100 ng/ml SDF-1α was added into the bottom chamber as a chemoattractant. The percentage of cells migrated into the bottom chamber 4 h later is shown. (F) Lin$^-$ BM cells were cultured at 37°C for 2 h in CH-296–coated 96-well plates containing IMDM supplemented with 10% FBS. Nonadherent cells were removed, and the percentage of adherent cells is shown. Cells used in this figure were isolated from poly I:C–injected *RhoA*$^{fl/fl}$; *Mx-Cre*$^+$ or *Mx-Cre*$^-$ mice. Numbers of samples analyzed: three (D and F) or four (E) mice per group. The results from a representative experiment of two (A–E) or four (F) independent experiments are shown. Error bars indicate SEM. *, $P < 0.05$.

Interestingly, a significant accumulation of G_2/M HPCs upon *RhoA* deletion was observed (Fig. 6 A). Recent genetic studies have emphasized the critical function of RhoA during mitosis in different biological contexts (Jackson et al., 2011; Melendez et al., 2011). To examine whether mitosis is defective in the *RhoA*-deficient HPCs, we purified LK cells and morphologically analyzed their nuclear contents. Similar to what has been reported in keratinocytes and mouse embryonic fibroblasts (Jackson et al., 2011; Melendez et al., 2011), *RhoA* deficiency resulted in an ∼10-fold elevation of multinucleated cells (Fig. 6 C). The nuclei were well separated but not condensed, suggesting that cytokinesis, rather than karyokinesis, was impaired. Indeed, a closer examination of 4N LK cells found a major accumulation of anaphase-like cells, which usually coincided with cytokinesis (Shuster and Burgess, 1999), whereas the frequency of metaphase cells was not significantly altered (Fig. 6 D), also suggesting a deficiency in later mitotic phases. Activation and localization of Aurora kinases, key mitotic-related kinases inactivating RhoA until anaphase (Andrews et al., 2003), were not affected by *RhoA* deficiency in all cell phases examined (Fig. 6 E), suggesting that the cytokinesis failure in response to *RhoA* deficiency is not caused by impaired Aurora kinase activity. These results indicate that RhoA is critical for regulating cytokinesis of hematopoietic progenitors through pathways other than Aurora kinase.

To dissect the downstream pathways involved in regulating cytokinesis of HPCs, we transduced control or *RhoA*-cKO LK cells with virus overexpressing either WT RhoA or effector binding–deficient mutant forms of RhoA, including E40L (ROCK binding deficient; Sahai et al., 1998), R68A (mDia binding deficient; Rose et al., 2005), and Y42C (protein kinase N [PKN] binding deficient; Sahai et al., 1998; Fig. 6 F). As predicted, expression of WT RhoA was able to rescue the accumulation of multinucleated cells (Fig. 6, G and H). Expression of Y42C-RhoA was also able to rescue the cytokinesis failure phenotype (Fig. 6, G and H), indicating RhoA–PKN interaction is not essential for cytokinesis. In contrast, expression of E40L and R68A RhoA was not sufficient to fully rescue the cytokinesis defects in *RhoA*-deficient cells (Fig. 6, G and H), indicating that both RhoA–ROCK and RhoA–mDia pathways are important for cytokinesis of HPCs.

RhoA deficiency causes programmed necrosis but not apoptosis or autophagy in the multipotent progenitor population

Regulation of apoptosis is essential for the maintenance of HSPCs (Domen and Weissman, 1999). Recent findings have indicated that molecules regulating autophagy, in addition to apoptosis, are also important for HSPC maintenance (Mortensen et al., 2011). Although necrosis has initially been postulated as an accidental and unregulated cellular event, accumulating evidence suggests that necrosis can also be tightly regulated (Galluzzi and Kroemer, 2008), but its molecular mechanism remains elusive and its role in the maintenance of HSPCs remains unclear.

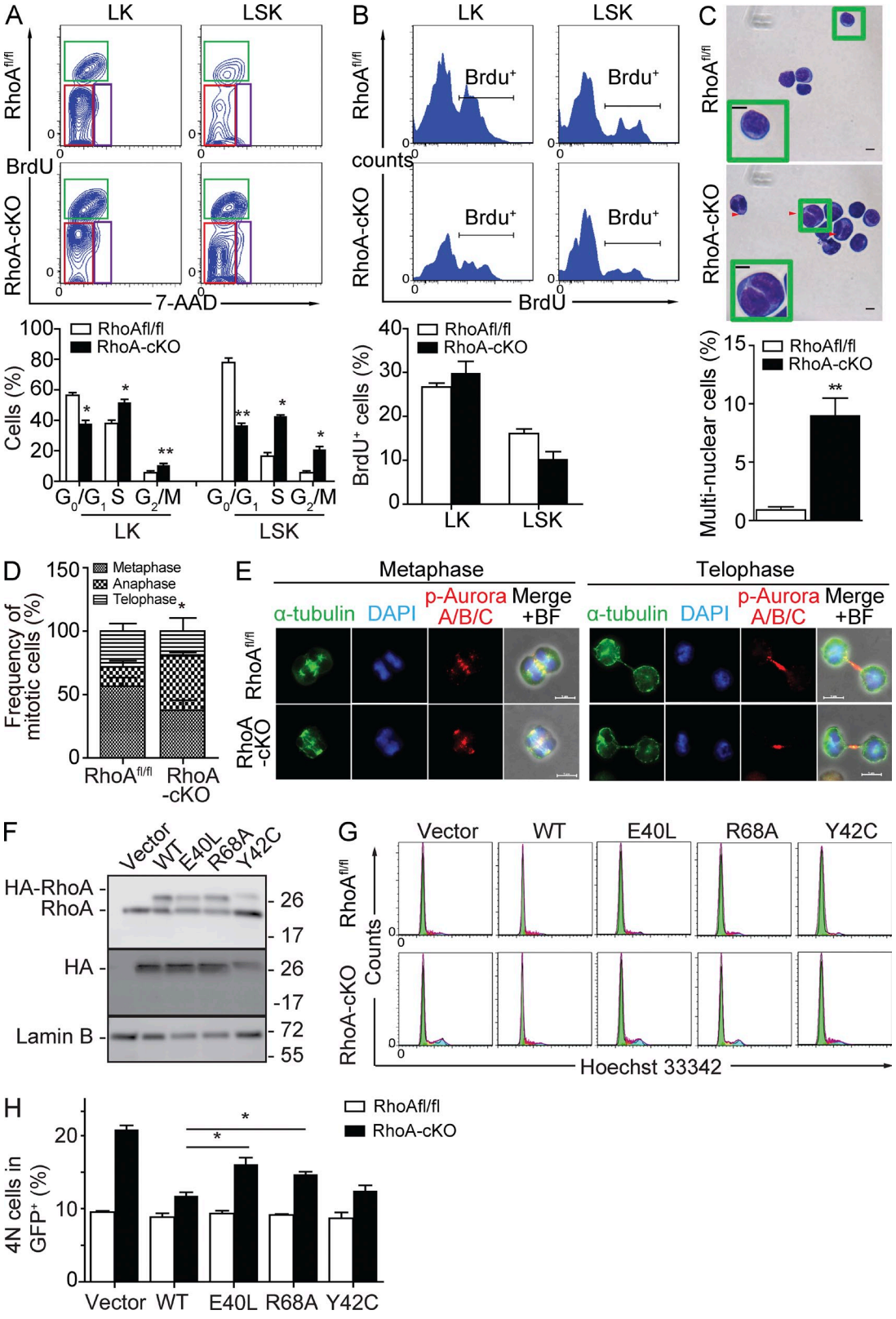

Figure 6. RhoA–ROCK and RhoA–mDia interactions are required for HPC cytokinesis. (A) Noncompetitive transplantation experiments were performed similarly as described in Fig. 1 G. A BrdU chase at 0.5 mg/recipient was performed 30 min before the analysis. Cell cycle distribution of LK and LSK cells in the noncompetitive transplanted recipients was examined by BrdU incorporation assay. (top) Representative flow cytometry plot. The red rectangle indicates G_0/G_1 phase, green rectangle S phase, and purple rectangle G/M phase. (bottom) Quantification of cell cycle distribution. (B) Competitive transplan-

The reduction of *RhoA*-null HPCs could be the result of decreased survival or other defects in response to cytokinesis failure. Consistent with a specific loss of LK cells, we observed a specific increase of cell death in the LK population (Annexin V/7-AAD staining; Fig. 7, A–C). In contrast, the frequency of cell death in the more primitive LSK population was not statistically different from the control group (Fig. 7, A–C). Similarly, in the competitive transplantation model, we observed an increase in cell death specifically in the donor-derived *RhoA*-null LK population, suggesting that increased death is intrinsic to the $RhoA^{-/-}$ HPC population. However, the survival of *RhoA*-null LSK cells was comparable with the WT control counterpart (not depicted). Thus, RhoA is critical in regulating survival of LK cells, but not the more primitive LSK population.

The majority of dead *RhoA*-null cells were observed in the 7-AAD^+ instead of Annexin V^+ population (Fig. 7, A–C), which was unusual and suggested that the increased cell death might not be caused by apoptosis because Annexin V^+ staining is a hallmark of apoptosis, whereas 7-AAD stains dead cells independently of the death mechanism. Consistent with this possibility, we found no evidence of caspase 3 cleavage in *RhoA*-null cells, by either Western blot or immunofluorescence (Fig. 7, D and E). Additionally, we did not observe a reduction of prosurvival signals such as Bcl-2, Bcl-xL, and Survivin or an increase of proapoptotic proteins such as p53 (Fig. 7 F), which was consistent with the involvement of a nonapoptotic cell death mechanism. There was also no change of the ratio between the two LC3B forms (Fig. 7 G), the hallmark of autophagy, suggesting that autophagy was not involved either. Electron microscopic examination of $RhoA^{-/-}$ Lin^- cells showed characteristics of necrosis, including the loss of membrane integrity and swelling of organelles (Fig. 7 H), suggesting that the increased death of $RhoA^{-/-}$ HPCs is related to increased necrosis. Although necrosis has been viewed as an accidental process, recent studies implicate pathways such as the TNF–receptor-interacting protein kinase (RIP) pathway as critical for regulating programmed necrosis (Vandenabeele et al., 2010). To examine whether the TNF–RIP pathway was altered in *RhoA*-null HPCs, we probed for expression of genes of this pathway. We noticed increased mRNA levels of molecules involved in the TNF–RIP pathway, including *Tnfα*, *Ripk3*, *Ferritin H1* (*Fth1*), and *Glud1* in *RhoA*-cKO LK cells (Fig. 7 I; Vandenabeele et al., 2010), suggesting that *RhoA* deficiency is associated with an increase of TNF–RIP-mediated programmed necrosis cascade. Interestingly, we observed a strong positive correlation between necrosis and mitotic failure (Fig. 7 J), implying that these cellular defects are closely associated. Finally, in addition to rescuing multilineage hematopoiesis potential (Fig. 4 F), expressing WT RhoA was also able to rescue the increased necrosis phenotype within $RhoA^{-/-}$ LK population in the competitive transplant setting (Fig. 7 K).

DISCUSSION

Rho family GTPases are well recognized intracellular signaling molecules, integrating a variety of signals to regulate multiple cellular processes, including cytoskeleton arrangement, gene expression, and cell cycle progression (Jaffe and Hall, 2005). The Rho GTPases Rac1, Rac2, RhoH, and Cdc42 have been genetically demonstrated to be uniquely involved in HSPC maintenance and homing/engraftment activities (Gu et al., 2003; Cancelas et al., 2005; Yang et al., 2007a,b; Chae et al., 2008). A previous study using a dominant-negative mutant of RhoA overexpression approach found that inhibition of RhoA activity enhanced HSPC proliferation and engraftment activities (Ghiaur et al., 2006). However, general concerns about a dominant-negative mutant overexpression approach, including a lack of specificity and dosage dependency and thus questionable physiological relevance, complicate a clear interpretation of such studies. Models in which RhoA is genetically deleted are valid experimental systems to define the role of RhoA in tissue/cell type–specific functions under physiological conditions.

RhoA is best appreciated as a key regulator of actomyosin, the signal effects of which are involved in adhesion, migration, mitosis, and gene expression. RhoA regulates actin polymerization through mDia and ROCK (Narumiya et al., 1997). Additionally, RhoA is critical for the spatial organization of actin filaments through ROCK- and citron kinase–mediated MLC phosphorylation (Yamashiro et al., 2003; Matsumura, 2005). In this study, we found that RhoA deficiency in HPCs

tations were performed similarly as described in Fig. 3. Samples were analyzed 5 mo after secondary transplantation. BrdU injection at 0.5 mg/recipient was performed 30 min before experiment. G_1-S transition of LK and LSK cells in the competitive transplanted recipients was examined by BrdU incorporation assay. (top) Representative flow cytometry plot. (bottom) Quantification of $BrdU^+$ cells. (C) Nuclei contents of LK cells. LK cells were FACS isolated 3 d after two poly I:C injections, and Giemsa staining was performed to determine nuclei contents. (top) Representative Giemsa staining. (bottom) Quantification of multinucleated cell frequency. Insets show enlarged representative cells. Red arrowheads indicate multinuclear cells. (D) LK cells were isolated from $RhoA^{fl/fl}$ or *RhoA*-cKO mice 3 d after two consecutive poly I:C injections. More than 30 mitotic cells per group were analyzed by morphology and DNA staining. Data were statistically analyzed by the χ^2 test. (E) Activation and distribution of Aurora A/B/C within LK cells. Cells were isolated 3 d after induction. The representative metaphase and telophase cells are shown. BF, brightfield. (F) Control or *RhoA*-cKO LK cells isolated 3 d after induction were transduced with mock retrovirus (REW13) or retrovirus expressing WT or effector binding–deficient mutant forms (E40L, R68A, and Y42C) of RhoA. Exogenous expression of RhoA was detected by both RhoA (top) and HA (middle) antibodies. Exogenous HA-RhoA mobilizes more slowly than endogenous RhoA because of the N-terminal 3x HA tag. Molecular masses (kilodaltons) are indicated to the right of the blots. (G and H) Percentage of 4N cells after expressing WT or mutant forms of RhoA. DNA contents were analyzed by Hoechst 33342 staining. (G) Representative flow cytometry plot. (H) Quantification of 4N cell frequency. Numbers of samples analyzed: four ($RhoA^{fl/fl}$) and five (*RhoA*-cKO; A), seven per group (B), four ($RhoA^{fl/fl}$) and six (*RhoA*-cKO; C), and three per group (D and H). (A–H) The results from a representative experiment of two independent experiments are shown. Error bars indicate SEM. *, $P < 0.05$; **, $P < 0.01$. Bars, 5 µm.

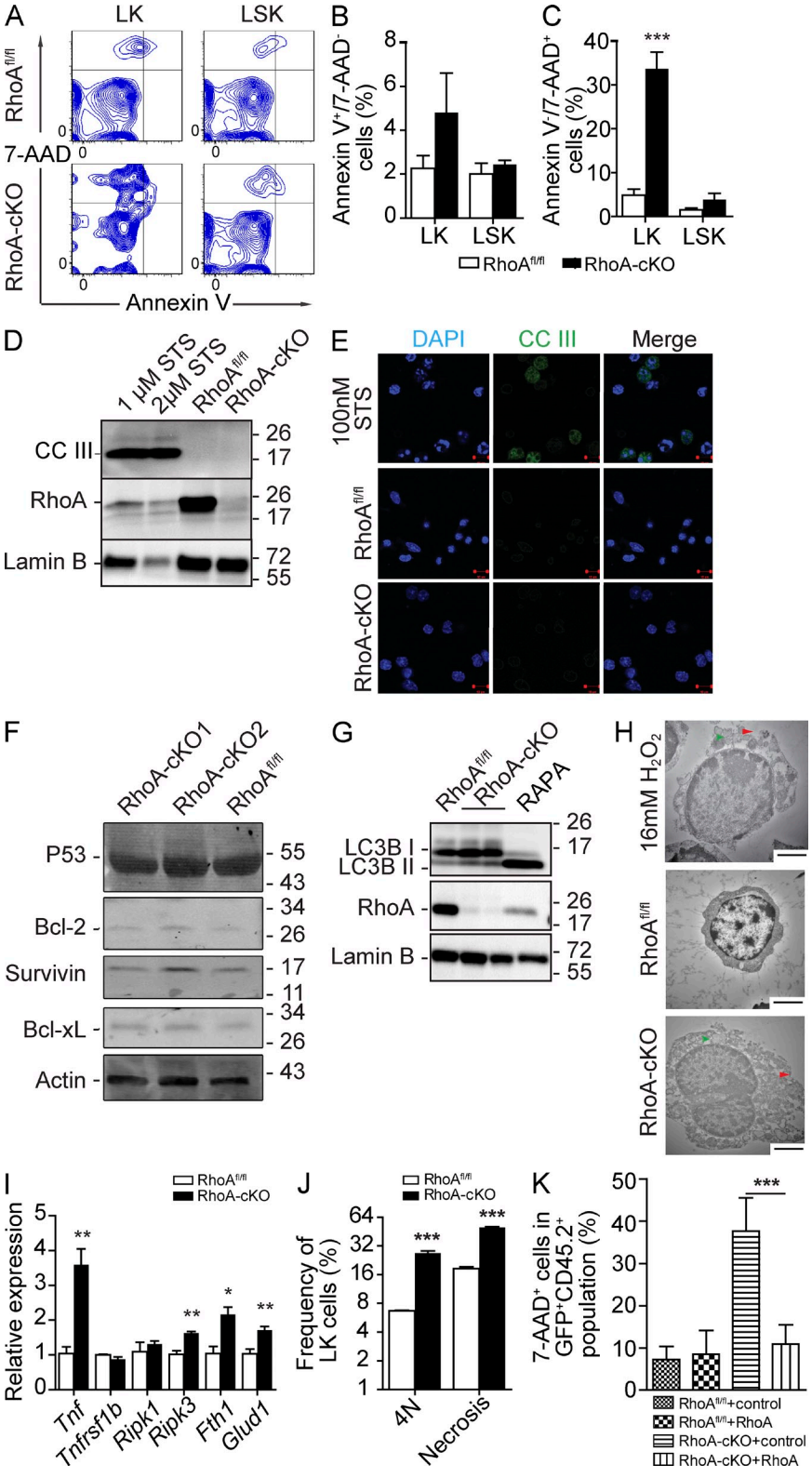

Figure 7. *RhoA* deficiency causes HPC necrosis but not apoptosis. (A–C) Congenic transplantation recipients described in Fig. 1 G were used, and BM cells were isolated 3 d after poly I:C induction. Cells were gated on the LK and LSK populations and analyzed by flow cytometry for Annexin V/7-AAD staining (A), apoptotic cells (B), and dead cells (C). (D) Cleavage of caspase 3 (CCIII) in Lin$^-$ cells of *RhoA*$^{fl/fl}$; *Mx-cre*$^+$ or *Mx-cre*$^-$ mice. Lin$^-$ cells were isolated 3 d after poly I:C injections. Staurosporine (STS)-treated WT Lin$^-$ cells were used as a positive apoptosis control. (E) CCIII staining of isolated LK cells. (F) p53, Bcl-xL, Bcl-2, and Survivin expression in Lin$^-$ cells of *RhoA*$^{fl/fl}$; *Mx-cre*$^+$ or *Mx-cre*$^-$ mice. Protein levels of apoptotic-related proteins were determined at 3 d after induction. (G) Levels of LC3B isoforms in Lin$^-$ cells of *RhoA*$^{fl/fl}$; *Mx-cre*$^+$ or *Mx-cre*$^-$ mice. Lin$^-$ cells were isolated 3 d after poly I:C injections. 100 nM Rapamycin (RAPA)–treated WT Lin$^-$ cells were used a positive autophagy control. (D, F, and G) Molecular masses (kilodaltons) are indicated to the right of the blots. (H) Representative electron micrographs of Lin$^-$ cells in native mice. 16 mM H_2O_2–treated Lin$^-$ cells were used as a positive necrosis control. Red arrowheads indicate features of membrane integrity loss. Green arrowheads indicate enlarged organelles. (I) Expression of TNF–RIP-related genes in LK cells 3 d after induction. (J) Association between cytokinesis failure (4N) and increased necrosis (7-AAD$^+$) in *RhoA*-deficient HPCs. BM Lin$^-$ cells were isolated at 3 d after induction. (K) Necrosis analysis of LK cells from recipients transplanted with LSK cells reconstituted with exogenous RhoA as described in Fig. 4 F. Numbers of samples analyzed: three (B, C, and J) or four (I and K) per group. (A–K) The results from a representative experiment of two independent experiments are shown. Error bars indicate SEM. *, $P < 0.05$; **, $P < 0.01$; ***, $P < 0.001$. Bars: (E) 10 μm; (H) 2 μm.

results in reduced MLC activity, yet RhoA signaling is dispensable for F-actin microfilament polymerization. We found that cytokinesis and migration, two cellular processes using myosin machinery as a driving force, are defective upon *RhoA* deletion. Together with data from other *RhoA* cKO models, our results highlight the diverse and context-dependent functions of RhoA and the uniqueness of RhoA GTPase in the primitive hematopoietic compartment. The findings suggest

that despite the commonalities shared by different Rho GTPases, such as structures, regulators, and effectors, the physiological function of each Rho GTPase can be unique and context specific.

In the present study, we demonstrate that *RhoA* is critical for multilineage hematopoiesis, the regulation of mitosis of HPCs, and the survival of the progenitors via regulation of programmed necrosis. Recent studies are consistent with our findings of a critical, but cell type–specific role for RhoA in hematopoiesis, in which a role of RhoA in the terminal differentiation of mature hematopoietic cells has been shown. Deletion of *RhoA* in B cells using *CD19*-Cre blocks B cell differentiation without affecting proliferation (Zhang et al., 2012). Megakaryocyte-specific *RhoA* deletion using *PF4*-Cre causes macrothrombocytopenia and generates defective platelets (Pleines et al., 2012). Additionally, our unpublished data using T cell– and erythroid-specific *RhoA* KO models indicate that RhoA is critical for T and red blood cell differentiation and function, although via different mechanisms at different cell differentiation stages. It will be of great interest to characterize the function of RhoA in other hematopoietic lineages using the cKO genetic models.

One striking finding of our study is that RhoA is absolutely required in HPC survival and the subsequent production of mature blood cells, but it is dispensable for the long-term maintenance of HSCs. RhoA, to our knowledge, is the first molecule identified to be specifically required for the regulation of multilineage progenitor cells but not the stem cells. There are several possible mechanisms accounting for this differential requirement of RhoA. Although no increased activity/expression of closely related RhoB/RhoC was observed upon *RhoA* deficiency, endogenous RhoB/RhoC activities might be sufficient to maintain the stem cells but not enough to rescue the deficiency of RhoA in HPCs. Alternatively, the different behaviors of $RhoA^{-/-}$ HSCs and HPCs could reflect the intrinsic difference between the two cell populations. Additional signals within the HSC population might not need RhoA signaling, but the RhoA pathways are turned on upon HSC differentiation to HPCs. Should this be the case, it will be interesting to identify the signaling pathways responsible for this difference. Another possibility is that the difference between *RhoA*-null HSCs and HPCs may come from the distinct cell cycle division kinetics and history of the two populations. Therefore, the faster and/or more divisions a cell goes through, the higher the likelihood of its experiencing a cytokinesis failure in response to loss of RhoA. Because HPCs commonly go through faster and more cell cycles than stem cells, they could more be vulnerable to cytokinesis failure.

Previous studies on endomitotic megakaryocytes suggest that the generation of 4N megakaryocytes from 2N cells is caused by the failure of the MLC-driven late ingression rather than the initial formation of cleavage furrow, which is followed by a backward movement and refusion of the two daughter cells (Geddis et al., 2007; Lordier et al., 2008). Similar to the endomitosis of megakaryocytes, in the *RhoA*-null HPCs we have observed a significant accumulation of anaphase cells, rather than metaphase or telophase cells. Interestingly, nuclei of the phenotypic anaphase cells are surrounded by Lamin B–labeled nuclear envelopes (unpublished data), which should only reform during or after telophase, suggesting the accumulation of anaphase cells is not because of blockage at the anaphase–telophase transition but rather is likely caused by a regression of cleavage furrow during cytokinesis. Whether the suppression of MLC activity in response to the loss of RhoA in HPCs directly contributes to the cytokinesis failure phenotype, as described for megakaryocytes, will need to be further investigated.

Cytokinesis failure can trigger aberrant segregation of chromosomes and activate cell death pathways (Castedo et al., 2004a,b). Increased necrosis, but not apoptosis or autophagy, is observed coinciding with the cytokinesis failure after *RhoA* deficiency. Differing from megakaryocytes, which undergo endomitosis and presumably obtain a unique mechanism to sustain survival, HPCs are normally diploid and lack the ability to withstand the stress from polyploidy and therefore undergo cell death. Consistent with the possibility that RhoA loss may induce a genomic stress from polyploidy of the cytokinesis blockage, a transcriptome analysis revealed an increase of the expression of DNA damage/repair pathway genes in the *RhoA*-null LK population (unpublished data). Interestingly, the correlating result of such cytokinesis arrest and genomic stress from the loss of RhoA is manifested by overexpression of multiple components of the TNF–RIP-mediated program necrosis pathway and phenotypic necrosis, rather than apoptosis or autophagy. Although poly I:C used in this study to induce the deletion of *RhoA* is known to trigger a transient increase of TNF–RIP-mediated necrosis (Penning et al., 1998), the observed necrosis after *RhoA* deficiency is not caused by a side effect of poly I:C treatment. In the competitive transplantation model, an increase of necrosis in the HPC population is observed 5 mo after secondary transplantation when any poly I:C effects should have been long gone. We conclude that the TNF–RIP-mediated necrosis of HPCs may be a consequence of *RhoA* deficiency and cytokinesis arrest.

In summary, we demonstrate that *RhoA* deficiency leads to acute BM failure and pan-cytopenia. *RhoA* signaling is required for HPC cell cycle progression but not HSC engraftment, and deletion of *RhoA* results in cytokinesis failure in HPCs. Interactions between RhoA and its downstream effectors ROCK and mDia appear to be critical signaling events as interruption of these interactions cause cytokinesis arrest. Cytokinesis failure in HPCs in response to the loss of RhoA is followed by programmed necrosis possibly involving TNF–RIP signaling. It is likely that RhoA-regulated HPC cytokinesis and the associated programmed necrosis are an underlying mechanism of HPC homeostasis and that HSCs and HPCs are equipped with distinct mechanisms involving RhoA to control cell division and death.

MATERIALS AND METHODS

Mice. C57BL/6 × B129 mixed background $RhoA^{fl/fl}$ mice were generated as previously described (Melendez et al., 2011) and crossed with *Mx-cre* mice. 6–8-wk-old *Mx-Cre*$^{+}$$RhoA^{fl/fl}$ and *Mx-cre*$^{-}$$RhoA^{fl/fl}$ mice were used throughout

this study. Two to three doses of poly I:C (Amgen Inc.) were administrated intraperitoneally to both mutant and littermate control mice on alternate days (10 µg/gram body weight). Time points are expressed as days after the final injection. Mice were bred and housed in a pathogen-free facility at Cincinnati Children's Hospital Medical Center in compliance with the Cincinnati Children's Hospital Medical Center Animal Care and Use Committee protocols.

Transplantation assays. For congenic transplantation experiments, 3×10^6 BM cells from CD45.2$^+$ *RhoA*$^{fl/fl}$ Mx-cre$^+$ or Mx-cre$^-$ mice were transplanted into lethally irradiated CD45.1$^+$ C57BL/6J WT recipients through the tail vein. After 8 wk of hematopoiesis, recipients were subjected to poly I:C injections, and samples were collected for analysis. Experiments were replicated twice.

For competitive transplantation experiment, 3×10^6 CD45.2$^+$ *RhoA*$^{fl/fl}$ Mx-cre$^+$ or Mx-cre$^-$ BM cells were mixed with an equal amount of CD45.1$^+$ WT BM cells and transplanted into lethally irradiated CD45.1$^+$ BoyJ WT recipients via the tail vein. After 8 wk, three doses of poly I:C were administrated, and PB samples were collected monthly for chimeric analysis. 4 mo after the poly I:C induction, recipients were sacrificed and 3×10^6 BM cells were transplanted into lethally irradiated secondary BoyJ recipients. PB chimerisms were checked monthly in the secondary recipients for at least 4 mo. Experiments were repeated three times, and at least four recipients were used for each genotype for each experiment.

For in vivo rescue experiments, lethally irradiated CD45.1$^+$ primary recipients were reconstituted with 3×10^6 CD45.2$^+$ *RhoA*$^{fl/fl}$ Mx-cre$^+$ or Mx-Cre$^-$ donor BM cells together with an equal amount of CD45.1$^+$ WT competitor BM cells. Three poly I:C injections were administered 6 wk after transplantation, and PB samples were collected to ensure *RhoA* deletion had occurred in the CD45.2$^+$ *RhoA*$^{fl/fl}$ Mx-cre$^+$ (in contrast to intact RhoA in the *RhoA*$^{fl/fl}$ Mx-cre$^-$) donor–derived cells, whereas CD45.1$^+$ competitor–derived cells were not affected. These primary recipients were sacrificed, and BM LSK and LK cells were isolated via immune-magnetic separation and FACS. LSK cells were transduced with a lentivirus vector expressing human RhoA and eGFP cDNA, or the control eGFP cDNA, driven by a ubiquitously expressing modified viral promoter, MND (Challita et al., 1995). In brief, LSK cells (mixture of CD45.2$^+$ donor cells and CD45.1$^+$ competitor cells) were prestimulated overnight in StemSpan SFEM medium (STEMCELL Technologies) supplemented with 2% fetal calf serum, 1% penicillin/streptomycin, 50 ng/ml recombinant murine SCF (rmSCF), 10 ng/ml mouse IL-3 (mIL-3), 1 mM deoxyribonucleotide triphosphate (dNTP), and 40 µg/ml low-density lipoprotein LDL (Sigma-Aldrich). LSK cells were transduced with either RhoA- or GFP-expressing lentivirus vector at a multiplicity of infection of 25, twice separated by 8–12 h. Sorted LK cells were also cultured separately under the same cytokine conditions without any viral transduction. Approximately 10,000-20,000 transduced LSK cells were cotransplanted with ∼25,000–50,000 untransduced irradiated LK cells as carrier cells into lethally irradiated CD45.1$^+$ secondary recipients. PB and BM samples were obtained monthly to analyze CD45.2$^+$ cells of different hematopoietic lineages that expressed eGFP. Survival data shown in Fig. 7 K were obtained at 8 mo after transplantation. Experiments were performed twice, and at least four recipients were used for each condition for each experiment.

Hematologic analysis. Mice were anesthetized and bled through the tail vein into EDTA-coated tubes (BD). Complete blood counts were analyzed using Hemavet 850 (Drew Scientific). BM cytospin slides were stained using Hema3 system (Thermo Fisher Scientific). Bone, spleen, and liver tissues were fixed in 10% formalin and stained with H&E.

Flow cytometry. BM cells were flushed from long bones (tibias, femurs, and iliac crests) with PBS (Invitrogen) plus 1% heat-inactivated FBS, 50 U/ml penicillin, and 50 µg/ml streptomycin and filtered through a 45-µm cell strainer (BD) to obtain single-cell suspensions. Red blood cells were lysed with Cell Lysis Buffer (BD).

Antibodies used in this study include: biotin-labeled anti-B220 (RA3-6B2), CD3e (145-2C11), CD4 (RM4-5), CD8 (53-6.7), CD11b (M1/70), Gr-1 (RB6-8C5), Ter-119 (TER-119), APC-conjugated anti-BrdU, c-Kit (2B8), B220 (RA3-6B2), CD11b (M1/70), APC-Cy7–conjugated anti-CD45.2 (104) streptavidin, PE-conjugated anti–Sca-1 (D7), CD135 (A2F10.1), CD45.1 (A20), FITC-conjugated anti-CD41 (MWReg30), CD48 (HM48-1), CD45.2 (104), Percp-Cy5.5–conjugated streptavidin, PE-Cy7–conjugated anti–Sca-1 (D7), CD45.2 (104; BD), FITC-conjugated anti-CD34 (RAM34), FcγRII/III (93), APC-Cy7–conjugated anti-IL7R (A7R34; eBioscience), and PE-Cy7–conjugated anti-CD150 (TC15-12F12.2; BioLegend).

Cell cycle analysis was performed using Hoechst 33342 (Invitrogen), PI/RNase staining buffer, or BrdU Flow kit (BD). Apoptosis was analyzed using the Annexin V Apoptosis Detection kit (BD) according to the manufacturer's protocol. Cell death was detected by 7-AAD staining (BD). Cortical F-actin was stained by Alex Fluor 488–phalloidin (Invitrogen).

Flow cytometry analysis was performed using FACSCanto II, FACSCanto III, or LSR II cytometry (BD), and data were analyzed using either FACSDiva (BD) or FlowJo software (Tree Star). Cell cycle distribution was calculated by FlowJo software using the Watson model. ImageStream data were acquired using ImageStream flow cytometry (Amnis) using 40× objective, and data were analyzed using IDEAS software (Amnis).

Isolation of HSPCs. To isolation of HSCs and progenitors, Lin$^-$ cells were enriched using a Lineage Cell Depletion kit (Miltenyi Biotec) according to the product manual. Isolated cells were then stained with biotin-labeled B220, CD3e, CD4, CD8, CD11b, Gr1, and Ter119 antibodies, followed by APC-Cy7–streptavidin, PE-Cy7–Sca-1, APC-CD117, FITC-CD34, and PE-CD135 for isolation of different HSC populations or APC-Cy7–streptavidin, PE–Sca-1, APC-CD117, PE-Cy7–FcγRII/III, and FITC-CD34 for isolating different myeloid progenitor populations. The FACSAria II (BD) was used to perform the isolation.

Microscopy. For immunofluorescent microscopic experiments, FACS-isolated cells were cultured in Iscove's modified Dulbecco's medium (IMDM; Invitrogen) with 10% FBS, 50 U/ml penicillin, 50 µg/ml streptomycin, 100 ng/ml rmSCF, recombinant human thrombopoietin (rhTPO; PeproTech), and recombinant human granulocyte colony stimulating factor (rhG-CSF; Amgen Inc.) on CH-296 (Takara Bio Inc.)–coated coverslips overnight and then fixed with 4% paraformaldehyde (Electron Microscopy Sciences) at room temperature for 15 min. Fixed cells were permeabilized with 0.2% Triton-PBS for 20 min and stained with primary antibodies overnight and secondary antibodies for 1 h. Antibodies and dyes used include anti–α-tubulin (Sigma-Aldrich), anti–Lamin B (M-20; Santa Cruz Biotechnology, Inc.), anti–Cleaved Caspase 3, anti–phosphorylated Aurora A/B/C (Cell Signaling Technology), Alexa Fluor 488 goat anti–mouse IgG (H+L), goat anti–rabbit IgG (H+L), Alexa Fluor 555 donkey anti–goat IgG (H+L), and DAPI (Invitrogen). Samples were mounted using VECTASHIELD Mounting Medium (Vector Laboratories). Slides were imaged on an LSM710 LIVE Duo Confocal Microscope at 40×/1.1 LD C-Apochromat (water immersion) objective (Carl Zeiss) at room temperature using the LSM710 Point Scanner (Carl Zeiss). Images were taken and analysis using Zen 2011 software (Carl Zeiss).

For H&E and Hema3 staining, cells and tissues were mounted using Permount Mounting Medium (Thermo Fisher Scientific) and imaged on a Motic BA310 microscope (Ted Pella) using a CCIS EF-N Plan Achromatic 40×/0.65 and 100×/1.25 objectives at room temperature by Moticam 580 camera (Ted Pella). Images were taken using Mitic Image Plus (Ted Pella) software and processed using ImageJ software (National Institutes of Health).

For electron microscopic analysis, isolated Lin$^-$ cells were fixed by 2.5% glutaraldehyde (Electron Microscopy Sciences) in PBS overnight. Cells were embedded in low melting temperature agarose, postfixed in 2% osmium tetroxide with 1.5% potassium ferrocyanide, 4% uranyl acetate solution, and then dehydrated by a series of ethanol solution and propylene oxide. Fixed cells were embedded in resin (Embed 812; Electron Microscope Sciences). Ultrathin (90 nm) sections were prepared by an ultra-microtone (Ultra Cut E; Reichert-Jung), and electron microscopic pictures were taken using an electron microscope (H7600; Hitachi High-Technologies America).

In vitro viral transduction. For retrovirus production, REW13 empty vector or REW13 vectors overexpressing WT RhoA or effector binding mutant forms of RhoA (E40L,Y42C, and R68A) were transfected into HEK 293T cells using the calcium phosphatase precipitation method. Viral supernatant was harvested at days three and four of transfection. LK cells were cultured in IMDM supplemented with 10% FBS, 50 U/ml penicillin, 50 µg/ml streptomycin, 100 ng/ml rmSCF, rhTPO (PeproTech), and rhG-CSF (Amgen Inc.) for 2 d before transduction. Viral particles were enriched by 20 µg/ml recombinant fibronectin CH-296 (Takara Bio Inc.). Stimulated LK cells were transduced for 24 h and further cultured free of virus for an additional 24 h before analysis.

Colony-forming units assay. 50,000 BM cells were seeded in cytokine-supplemented MethoCult GF M3434 medium (STEMCELL Technologies) for 7 d, and colonies were enumerated based on size and morphology.

Adhesion and migration assays. For adhesion assay, 10^5 Lin^- cells were cultured at 37°C in CH-296–coated 96-well plates in 10% FBS supplemented IMDM for 2 h. Nonadherent cells were removed by 2× PBS wash. Adherent cells were recovered by 10-min trypsin treatment, and the number of adherent cells was counted.

For migration assay, 10^5 Lin^- cells were cultured in the top chamber of Transwell (Corning) in IMDM with 0.5% BSA (Sigma-Aldrich). 100 ng/ml SDF-1α (PeproTech) was added into the bottom chamber as a chemoattractant cue. 4 h later, cells migrated into the bottom chamber were collected for enumeration.

Protein activity and expression assays. For Rhotekin RBD pull-down assay, isolated Lin^- cells were starved overnight and stimulated with 10 ng/ml SCF or SDF-1α or transferred onto a 20 µg/ml CH-296–coated nontissue culture dish for 10 min at 37°C. GTP-bound RhoA was pulled down and analyzed using Rhotekin RBD Agarose Beads (Cell Biolab, Inc.) according to the product manual.

For protein expression analysis, isolated Lin^- cells were lysed by RIPA buffer (Cell Signaling Technology) according to the manufacturer's protocol. 10–50 µg of total protein was loaded depending on antigen level/antibody quality for Western blot analysis. Antibodies used include RhoA (67B9), RhoB, RhoC (D40E4), phosphor-MLC (Ser19), total MLC, phosphor-cofilin (Ser3), cofilin, Cleaved Caspase-3 (Asp175), Bcl-2, Bcl-xL, Survivin, p53, LC3B (Cell Signaling Technology), and Lamin B (M-20; Santa Cruz Biotechnology).

Transcript expression. Total RNA was extracted from FACS-isolated HSPCs using an RNeasy Micro kit (QIAGEN) according to the manufacturer's manual. Complementary DNA was generated using the High Capacity cDNA kit (Life Technologies). Mouse TaqMan assays used in this study were purchased from Applied Biosystems: *Tnf* (Mm00443260_g1), *Tnfsf1B* (Mm00441889_m1), *Ripk1* (Mm00436354_m1), *Ripk3* (Mm01319233_g1), *Hsp90aa1* (Mm00658568_gH), *Fth1* (Mm00850707_g1), *Glud1* (Mm00492353_m1), and *Gapdh* (Mm99999915_g1). All experiments were performed in triplicate using the ΔΔCt method, and differences in cDNA concentration were normalized against endogenous *Gapdh* level.

Data analysis. Results are shown as mean ± SEM from at least three individual experiments per group. Statistical analysis between control and *RhoA*-cKO was assessed by an unpaired, two-tail Student's *t* test except for the phase distribution of mitotic cells (Fig. 6 G), which is assessed by a χ^2 test. *, $P < 0.05$; **, $P < 0.01$; ***, $P < 0.001$, except for Fig. 3, in which *, $P < 0.001$.

We thank James F. Johnson, Lanxi Song, Kalpana Nattamai, and Ashwini Hinge for their technical help, and Drs. Paul Andreassen, Gang Huang, and James Mulloy for helpful discussions. We thank Zheng laboratory members for discussion and critiques.

This work was supported in part by National Institutes of Health grants R01CA150547, P30 DK090971, and R01AG040118 and the Deutsche Forschungsgemeinschaft KFO 142, GE2063/1, Forschungsprogramm "Internationale Spitzenforschung II/3" der Baden-Württemberg Stiftung P-BWS-SPII/3-06. X. Zhou is a PhD candidate at the University of Cincinnati, and this work is submitted in partial fulfillment of the requirement for the PhD degree.

The authors have no conflicting financial interests.

Submitted: 19 October 2012
Accepted: 9 September 2013

REFERENCES

Andrews, P.D., E. Knatko, W.J. Moore, and J.R. Swedlow. 2003. Mitotic mechanics: the auroras come into view. *Curr. Opin. Cell Biol.* 15:672–683. http://dx.doi.org/10.1016/j.ceb.2003.10.013

Arai, F., A. Hirao, M. Ohmura, H. Sato, S. Matsuoka, K. Takubo, K. Ito, G.Y. Koh, and T. Suda. 2004. Tie2/angiopoietin-1 signaling regulates hematopoietic stem cell quiescence in the bone marrow niche. *Cell.* 118:149–161. http://dx.doi.org/10.1016/j.cell.2004.07.004

Boggs, D.R., and S.S. Boggs. 1976. Editorial: The pathogenesis of aplastic anemia: a defective pluripotent hematopoietic stem cell with inappropriate balance of differentiation and self-replication. *Blood.* 48:71–76.

Bonnet, D., and J.E. Dick. 1997. Human acute myeloid leukemia is organized as a hierarchy that originates from a primitive hematopoietic cell. *Nat. Med.* 3:730–737. http://dx.doi.org/10.1038/nm0797-730

Broudy, V.C. 1997. Stem cell factor and hematopoiesis. *Blood.* 90:1345–1364.

Cancelas, J.A., A.W. Lee, R. Prabhakar, K.F. Stringer, Y. Zheng, and D.A. Williams. 2005. Rac GTPases differentially integrate signals regulating hematopoietic stem cell localization. *Nat. Med.* 11:886–891. http://dx.doi.org/10.1038/nm1274

Castedo, M., J.L. Perfettini, T. Roumier, K. Andreau, R. Medema, and G. Kroemer. 2004a. Cell death by mitotic catastrophe: a molecular definition. *Oncogene.* 23:2825–2837. http://dx.doi.org/10.1038/sj.onc.1207528

Castedo, M., J.L. Perfettini, T. Roumier, A. Valent, H. Raslova, K. Yakushijin, D. Horne, J. Feunteun, G. Lenoir, R. Medema, et al. 2004b. Mitotic catastrophe constitutes a special case of apoptosis whose suppression entails aneuploidy. *Oncogene.* 23:4362–4370. http://dx.doi.org/10.1038/sj.onc.1207572

Castor, A., L. Nilsson, I. Astrand-Grundström, M. Buitenhuis, C. Ramirez, K. Anderson, B. Strömbeck, S. Garwicz, A.N. Békássy, K. Schmiegelow, et al. 2005. Distinct patterns of hematopoietic stem cell involvement in acute lymphoblastic leukemia. *Nat. Med.* 11:630–637. http://dx.doi.org/10.1038/nm1253

Chae, H.D., K.E. Lee, D.A. Williams, and Y. Gu. 2008. Cross-talk between RhoH and Rac1 in regulation of actin cytoskeleton and chemotaxis of hematopoietic progenitor cells. *Blood.* 111:2597–2605. http://dx.doi.org/10.1182/blood-2007-06-093237

Challita, P.M., D. Skelton, A. el-Khoueiry, X.J. Yu, K. Weinberg, and D.B. Kohn. 1995. Multiple modifications in cis elements of the long terminal repeat of retroviral vectors lead to increased expression and decreased DNA methylation in embryonic carcinoma cells. *J. Virol.* 69:748–755.

Chauhan, B.K., M. Lou, Y. Zheng, and R.A. Lang. 2011. Balanced Rac1 and RhoA activities regulate cell shape and drive invagination morphogenesis in epithelia. *Proc. Natl. Acad. Sci. USA.* 108:18289–18294. http://dx.doi.org/10.1073/pnas.1108993108

Cheng, T., N. Rodrigues, D. Dombkowski, S. Stier, and D.T. Scadden. 2000a. Stem cell repopulation efficiency but not pool size is governed by p27(kip1). *Nat. Med.* 6:1235–1240. http://dx.doi.org/10.1038/81335

Cheng, T., N. Rodrigues, H. Shen, Y. Yang, D. Dombkowski, M. Sykes, and D.T. Scadden. 2000b. Hematopoietic stem cell quiescence maintained by p21cip1/waf1. *Science.* 287:1804–1808. http://dx.doi.org/10.1126/science.287.5459.1804

Domen, J., and I.L. Weissman. 1999. Self-renewal, differentiation or death: regulation and manipulation of hematopoietic stem cell fate. *Mol. Med. Today.* 5:201–208. http://dx.doi.org/10.1016/S1357-4310(99)01464-1

Galluzzi, L., and G. Kroemer. 2008. Necroptosis: a specialized pathway of programmed necrosis. *Cell.* 135:1161–1163. http://dx.doi.org/10.1016/j.cell.2008.12.004

Ganem, N.J., Z. Storchova, and D. Pellman. 2007. Tetraploidy, aneuploidy and cancer. *Curr. Opin. Genet. Dev.* 17:157–162. http://dx.doi.org/10.1016/j.gde.2007.02.011

Geddis, A.E., N.E. Fox, E. Tkachenko, and K. Kaushansky. 2007. Endomitotic megakaryocytes that form a bipolar spindle exhibit cleavage furrow ingression followed by furrow regression. *Cell Cycle*. 6:455–460. http://dx.doi.org/10.4161/cc.6.4.3836

Geh, E., Q. Meng, M. Mongan, J. Wang, A. Takatori, Y. Zheng, A. Puga, R.A. Lang, and Y. Xia. 2011. Mitogen-activated protein kinase kinase kinase 1 (MAP3K1) integrates developmental signals for eyelid closure. *Proc. Natl. Acad. Sci. USA*. 108:17349–17354. http://dx.doi.org/10.1073/pnas.1102297108

Ghaffari, S. 2008. Oxidative stress in the regulation of normal and neoplastic hematopoiesis. *Antioxid. Redox Signal*. 10:1923–1940. http://dx.doi.org/10.1089/ars.2008.2142

Ghiaur, G., A. Lee, J. Bailey, J.A. Cancelas, Y. Zheng, and D.A. Williams. 2006. Inhibition of RhoA GTPase activity enhances hematopoietic stem and progenitor cell proliferation and engraftment. *Blood*. 108:2087–2094. http://dx.doi.org/10.1182/blood-2006-02-001560

Gu, Y., M.D. Filippi, J.A. Cancelas, J.E. Siefring, E.P. Williams, A.C. Jasti, C.E. Harris, A.W. Lee, R. Prabhakar, S.J. Atkinson, et al. 2003. Hematopoietic cell regulation by Rac1 and Rac2 guanosine triphosphatases. *Science*. 302:445–449. http://dx.doi.org/10.1126/science.1088485

Hattori, K., B. Heissig, and S. Rafii. 2003. The regulation of hematopoietic stem cell and progenitor mobilization by chemokine SDF-1. *Leuk. Lymphoma*. 44:575–582. http://dx.doi.org/10.1080/1042819021000037985

Heasman, S.J., and A.J. Ridley. 2008. Mammalian Rho GTPases: new insights into their functions from in vivo studies. *Nat. Rev. Mol. Cell Biol.* 9:690–701. http://dx.doi.org/10.1038/nrm2476

Jackson, B., K. Peyrollier, E. Pedersen, A. Basse, R. Karlsson, Z. Wang, T. Lefever, A.M. Ochsenbein, G. Schmidt, K. Aktories, et al. 2011. RhoA is dispensable for skin development, but crucial for contraction and directed migration of keratinocytes. *Mol. Biol. Cell*. 22:593–605. http://dx.doi.org/10.1091/mbc.E09-10-0859

Jaffe, A.B., and A. Hall. 2005. Rho GTPases: biochemistry and biology. *Annu. Rev. Cell Dev. Biol.* 21:247–269. http://dx.doi.org/10.1146/annurev.cellbio.21.020604.150721

Janzen, V., R. Forkert, H.E. Fleming, Y. Saito, M.T. Waring, D.M. Dombkowski, T. Cheng, R.A. DePinho, N.E. Sharpless, and D.T. Scadden. 2006. Stem-cell ageing modified by the cyclin-dependent kinase inhibitor p16INK4a. *Nature*. 443:421–426.

Kiel, M.J., O.H. Yilmaz, T. Iwashita, O.H. Yilmaz, C. Terhorst, and S.J. Morrison. 2005. SLAM family receptors distinguish hematopoietic stem and progenitor cells and reveal endothelial niches for stem cells. *Cell*. 121:1109–1121. http://dx.doi.org/10.1016/j.cell.2005.05.026

Kimura, K., M. Ito, M. Amano, K. Chihara, Y. Fukata, M. Nakafuku, B. Yamamori, J. Feng, T. Nakano, K. Okawa, et al. 1996. Regulation of myosin phosphatase by Rho and Rho-associated kinase (Rho-kinase). *Science*. 273:245–248. http://dx.doi.org/10.1126/science.273.5272.245

Knoblich, J.A. 2008. Mechanisms of asymmetric stem cell division. *Cell*. 132:583–597. http://dx.doi.org/10.1016/j.cell.2008.02.007

Kozar, K., M.A. Ciemerych, V.I. Rebel, H. Shigematsu, A. Zagozdzon, E. Sicinska, Y. Geng, Q. Yu, S. Bhattacharya, R.T. Bronson, et al. 2004. Mouse development and cell proliferation in the absence of D-cyclins. *Cell*. 118:477–491. http://dx.doi.org/10.1016/j.cell.2004.07.025

Kühn, R., F. Schwenk, M. Aguet, and K. Rajewsky. 1995. Inducible gene targeting in mice. *Science*. 269:1427–1429. http://dx.doi.org/10.1126/science.7660125

Lordier, L., A. Jalil, F. Aurade, F. Larbret, J. Larghero, N. Debili, W. Vainchenker, and Y. Chang. 2008. Megakaryocyte endomitosis is a failure of late cytokinesis related to defects in the contractile ring and Rho/Rock signaling. *Blood*. 112:3164–3174. http://dx.doi.org/10.1182/blood-2008-03-144956

Maekawa, M., T. Ishizaki, S. Boku, N. Watanabe, A. Fujita, A. Iwamatsu, T. Obinata, K. Ohashi, K. Mizuno, and S. Narumiya. 1999. Signaling from Rho to the actin cytoskeleton through protein kinases ROCK and LIM-kinase. *Science*. 285:895–898. http://dx.doi.org/10.1126/science.285.5429.895

Matsumura, F. 2005. Regulation of myosin II during cytokinesis in higher eukaryotes. *Trends Cell Biol.* 15:371–377. http://dx.doi.org/10.1016/j.tcb.2005.05.004

Melendez, J., K. Stengel, X. Zhou, B.K. Chauhan, M. Debidda, P. Andreassen, R.A. Lang, and Y. Zheng. 2011. RhoA GTPase is dispensable for actomyosin regulation but is essential for mitosis in primary mouse embryonic fibroblasts. *J. Biol. Chem*. 286:15132–15137. http://dx.doi.org/10.1074/jbc.C111.229336

Min, I.M., G. Pietramaggiori, F.S. Kim, E. Passegué, K.E. Stevenson, and A.J. Wagers. 2008. The transcription factor EGR1 controls both the proliferation and localization of hematopoietic stem cells. *Cell Stem Cell*. 2:380–391. http://dx.doi.org/10.1016/j.stem.2008.01.015

Mortensen, M., A.S. Watson, and A.K. Simon. 2011. Lack of autophagy in the hematopoietic system leads to loss of hematopoietic stem cell function and dysregulated myeloid proliferation. *Autophagy*. 7:1069–1070. http://dx.doi.org/10.4161/auto.7.9.15886

Narumiya, S., T. Ishizaki, and N. Watanabe. 1997. Rho effectors and reorganization of actin cytoskeleton. *FEBS Lett*. 410:68–72. http://dx.doi.org/10.1016/S0014-5793(97)00317-7

Penning, L.C., R.G. Schipper, D. Vercammen, A.A. Verhofstad, T. Denecker, R. Beyaert, and P. Vandenabeele. 1998. Sensitization of tnf-induced apoptosis with polyamine synthesis inhibitors in different human and murine tumour cell lines. *Cytokine*. 10:423–431. http://dx.doi.org/10.1006/cyto.1997.0310

Piekny, A., M. Werner, and M. Glotzer. 2005. Cytokinesis: welcome to the Rho zone. *Trends Cell Biol.* 15:651–658. http://dx.doi.org/10.1016/j.tcb.2005.10.006

Pleines, I., I. Hagedorn, S. Gupta, F. May, L. Chakarova, J. van Hengel, S. Offermanns, G. Krohne, C. Kleinschnitz, C. Brakebusch, and B. Nieswandt. 2012. Megakaryocyte-specific RhoA deficiency causes macrothrombocytopenia and defective platelet activation in hemostasis and thrombosis. *Blood*. 119:1054–1063. http://dx.doi.org/10.1182/blood-2011-08-372193

Randall, T.D., and I.L. Weissman. 1997. Phenotypic and functional changes induced at the clonal level in hematopoietic stem cells after 5-fluorouracil treatment. *Blood*. 89:3596–3606.

Rose, R., M. Weyand, M. Lammers, T. Ishizaki, M.R. Ahmadian, and A. Wittinghofer. 2005. Structural and mechanistic insights into the interaction between Rho and mammalian Dia. *Nature*. 435:513–518. http://dx.doi.org/10.1038/nature03604

Sahai, E., A.S. Alberts, and R. Treisman. 1998. RhoA effector mutants reveal distinct effector pathways for cytoskeletal reorganization, SRF activation and transformation. *EMBO J.* 17:1350–1361. http://dx.doi.org/10.1093/emboj/17.5.1350

Shuster, C.B., and D.R. Burgess. 1999. Parameters that specify the timing of cytokinesis. *J. Cell Biol.* 146:981–992. http://dx.doi.org/10.1083/jcb.146.5.981

Storchova, Z., and D. Pellman. 2004. From polyploidy to aneuploidy, genome instability and cancer. *Nat. Rev. Mol. Cell Biol.* 5:45–54. http://dx.doi.org/10.1038/nrm1276

Van Aelst, L., and C. D'Souza-Schorey. 1997. Rho GTPases and signaling networks. *Genes Dev*. 11:2295–2322. http://dx.doi.org/10.1101/gad.11.18.2295

Vandenabeele, P., L. Galluzzi, T. Vanden Berghe, and G. Kroemer. 2010. Molecular mechanisms of necroptosis: an ordered cellular explosion. *Nat. Rev. Mol. Cell Biol.* 11:700–714. http://dx.doi.org/10.1038/nrm2970

Venezia, T.A., A.A. Merchant, C.A. Ramos, N.L. Whitehouse, A.S. Young, C.A. Shaw, and M.A. Goodell. 2004. Molecular signatures of proliferation and quiescence in hematopoietic stem cells. *PLoS Biol.* 2:e301. http://dx.doi.org/10.1371/journal.pbio.0020301

Wang, L., and Y. Zheng. 2007. Cell type-specific functions of Rho GTPases revealed by gene targeting in mice. *Trends Cell Biol.* 17:58–64. http://dx.doi.org/10.1016/j.tcb.2006.11.009

Xiang, S.Y., D. Vanhoutte, D.P. Del Re, N.H. Purcell, H. Ling, I. Banerjee, J. Bossuyt, R.A. Lang, Y. Zheng, S.J. Matkovich, et al. 2011. RhoA protects the mouse heart against ischemia/reperfusion injury. *J. Clin. Invest*. 121:3269–3276. http://dx.doi.org/10.1172/JCI44371

Yamashiro, S., G. Totsukawa, Y. Yamakita, Y. Sasaki, P. Madaule, T. Ishizaki, S. Narumiya, and F. Matsumura. 2003. Citron kinase, a Rho-dependent kinase, induces di-phosphorylation of regulatory light chain of myosin II. *Mol. Biol. Cell*. 14:1745–1756. http://dx.doi.org/10.1091/mbc.E02-07-0427

Yang, L., L. Wang, H. Geiger, J.A. Cancelas, J. Mo, and Y. Zheng. 2007a. Rho GTPase Cdc42 coordinates hematopoietic stem cell quiescence and niche interaction in the bone marrow. *Proc. Natl. Acad. Sci. USA*. 104:5091–5096. http://dx.doi.org/10.1073/pnas.0610819104

Yang, L., L. Wang, T.A. Kalfa, J.A. Cancelas, X. Shang, S. Pushkaran, J. Mo, D.A. Williams, and Y. Zheng. 2007b. Cdc42 critically regulates the balance between myelopoiesis and erythropoiesis. *Blood*. 110:3853–3861. http://dx.doi.org/10.1182/blood-2007-03-079582

Yilmaz, O.H., R. Valdez, B.K. Theisen, W. Guo, D.O. Ferguson, H. Wu, and S.J. Morrison. 2006. Pten dependence distinguishes haematopoietic stem cells from leukaemia-initiating cells. *Nature*. 441:475–482. http://dx.doi.org/10.1038/nature04703

Yoder, M.C., and D.A. Williams. 1995. Matrix molecule interactions with hematopoietic stem cells. *Exp. Hematol*. 23:961–967.

Zhang, J., J.C. Grindley, T. Yin, S. Jayasinghe, X.C. He, J.T. Ross, J.S. Haug, D. Rupp, K.S. Porter-Westpfahl, L.M. Wiedemann, et al. 2006. PTEN maintains haematopoietic stem cells and acts in lineage choice and leukaemia prevention. *Nature*. 441:518–522. http://dx.doi.org/10.1038/nature04747

Zhang, S., X. Zhou, R.A. Lang, and F. Guo. 2012. RhoA of the Rho family small GTPases is essential for B lymphocyte development. *PLoS ONE*. 7:e33773. http://dx.doi.org/10.1371/journal.pone.0033773

Zou, P., H. Yoshihara, K. Hosokawa, I. Tai, K. Shinmyozu, F. Tsukahara, Y. Maru, K. Nakayama, K.I. Nakayama, and T. Suda. 2011. p57(Kip2) and p27(Kip1) cooperate to maintain hematopoietic stem cell quiescence through interactions with Hsc70. *Cell Stem Cell*. 9:247–261. http://dx.doi.org/10.1016/j.stem.2011.07.003